THE MEASUREMENT OF THE INFLUENCE OF THE ADHESION LOSS ON THE DYNAMIC LOAD OF THE DRIVE REACTION ROD ON THE ROLLER RIG

Vojtěch Dybala

Czech Technical University in Prague, Faculty of Mechanical Engineering, Department of Automotive, Combustion Engines and Railway Engineering, Technická 4, 160 07 Prague, Czech Republic

correspondence: `vojtech.dybala@fs.cvut.cz`

Abstract. The dynamic behaviour and dynamic phenomena in traction drives of railway vehicle has been studied for decades. Generally, in these days the motivation for this research is to look for answers related with service problems, which has been risen, e.g. an overloading of mechanical components as wheelsets or an intention to improve control systems of traction drives of railway vehicles. This problematic has also motivated the research at the Faculty of Mechanical Engineering at the Czech Technical University (CTU) in Prague. Nowadays it is also usual, that the main research tool has been a simulation based on a mathematical model of a railway vehicle or its specific components, as testing on real vehicles is very demanding regarding costs. However, there is an alternative – a roller rig. At the CTU in Prague there has been modernized the second roller rig for purposes of measurement regarding the torsion dynamics research, to support PhD students for their theses and possibly to extend the education for students oriented on the railway vehicle's design. This contribution brings results of measurements just from the problematics of torsion oscillations and dynamics. Specifically, further presented measurements are on the loss of the adhesion in the contact of the wheelset and rollers, as the substitution for the railway, its impact on the reaction rod overloading and study of the axle load influence on the transition phenomena.

Keywords: Railway vehicle, torsion, adhesion, roller rig, wheel-rail contact.

1. Introduction

Within the construction of the railway vehicle the traction drive is a big functional system, generally it is an electro-mechanical system. In these terms the electrical part is intended to be from a pantograph to an electromagnetical circuit of a traction motor. The mechanical part then is from a rotor of the traction motor to a contact of a wheelset and a rail. Further is dealt with the mechanical part for purposes of this contribution.

From the conceptual perspective the mechanical part of traction drive is divided into three groups:

- Axle-hung drive (Figure 1),
- Partly-suspended drive (Figure 2),
- Fully-suspended drive (Figure 3).

These three groups differ in the amount of the mass, which is connected to a wheelset (unsuspended mass) and to a bogie frame (primarily suspended mass).

The applicability for a specific vehicle is generally derived from the supposed maximal service speed of the vehicle and needs to reduce the dynamic interaction between the wheelset and the track via reduction of mass connected to the wheelset. It can be defined, that the axle hung drive is typical for slower vehicles with the maximal service speed of $140/160 \, \mathrm{km \, h^{-1}}$, the partly-suspended drive for maximal service speeds from up to $190 \, \mathrm{km \, h^{-1}}$ and high-speed vehicles as
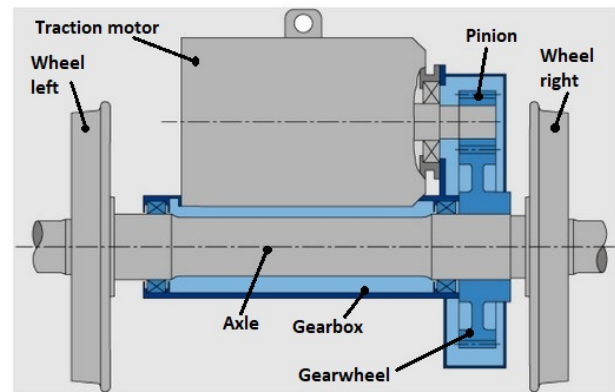

Figure 1. An axle-hung drive [1].

defined by the TSI and fully-suspended drives for medium and high-speed applications as well.

From the perspective of this contribution the first two types of drive are in question as they utilize a specific design feature – a reaction rod, see Figure 4.

The function of the reaction rod is to connect the traction gearbox or the drive to the bogie frame and realize a support for reaction force (S), which comes from traction forces in the wheel-rail contact (T) and forces from vertical dynamics, given by track irregularities. The reaction rod can be realized as vertical, horizontal or generally inclined (Figure 5).

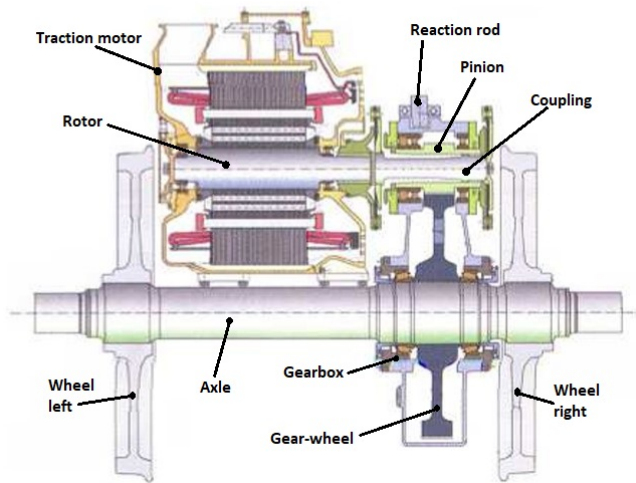The reaction rod is the component, which needs to
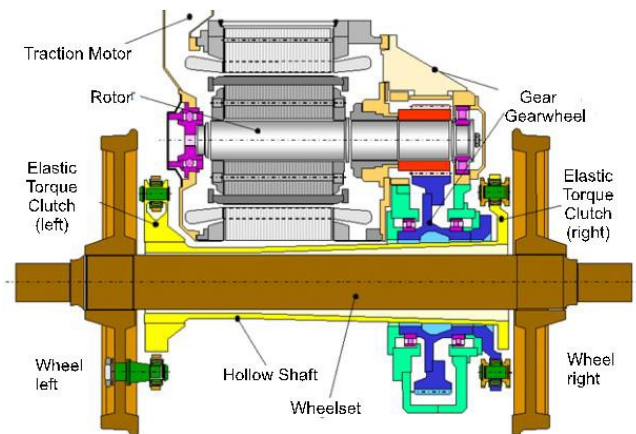
FIGURE 2. A partly-suspended drive of a locomotive [2].

FIGURE 4. A traction gearbox with a vertical reaction rod [3].

FIGURE 3. A fully-suspended drive of a locomotive [2].
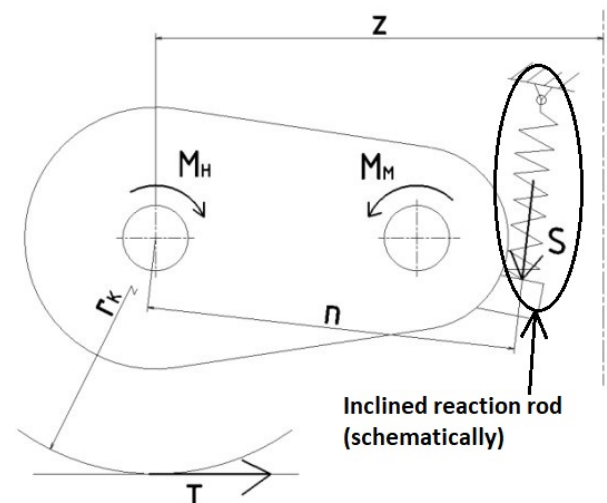
FIGURE 5. Inclined reaction rod – schematics [3].

be considered within mathematical models for simulations as well. Nowadays there are many publications, which describes mathematical models with implemented reaction rod, how to model it and its influences within simulations [4–8]. For this contribution important has been the thesis of Martin Dub [9], which provides also results of practical measurements on reaction rods of rail vehicles. In both cases, tramcar 14T (Figure 6) and metro car (Figure 7), the measurements proved the suitability of a reaction rod as a diagnostic feature to investigate bogie assembly and its failure modes during service.

If this work proved sufficient sensitivity of a reaction rod for utilization as an auto diagnostic feature it also raises a question if it could be a good part to measure a transition phenomenon of a loss and re-gain of the adhesion in the wheel-rail contact and its influence due to overloading of the reaction rod.

2. Reaction Rod of Roller Rig

For purposes of measurement of vertical wheel forces and longitudinal tractive and brake forces the second roller rig of CTU in Prague has been modernized so,
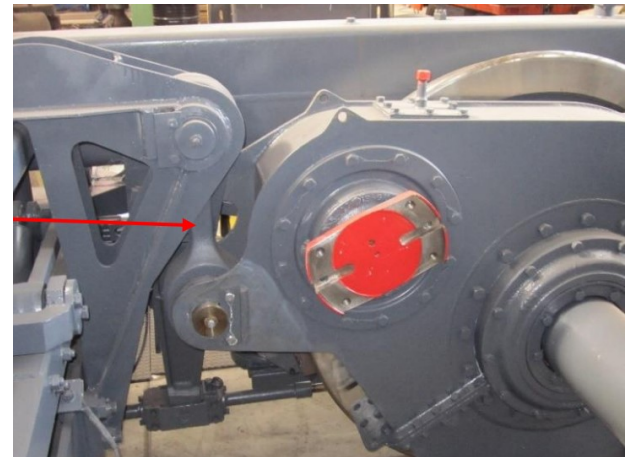
that measuring rods and beams has been equipped by strain gauges, see Figure 8.

The reaction rod on the roller rig is inclined horizontal rod (Figure 9). Because the drive of the wheelset is an axle-hung type the function between the tangential force in the wheel-roller contact T1 and the force S1, which loads the reaction rod itself, is defined by the Equation (1).

$$S_1 = T_1 \frac{r_{DV}}{n} . \qquad (1)$$

In principle the Equation (1) defines, that any longitudinal force (static, dynamic, transitional) acting in the wheel-roller contact should be measurable via the reaction rod, if the reaction rod has a sufficient sensitivity – flexibility. As the roller rig is disproportional in terms of dimensions, weights and installed power the measuring rods has reduced dimensions of shank with squared cross-section of side length of 5 mm – Figure 10.
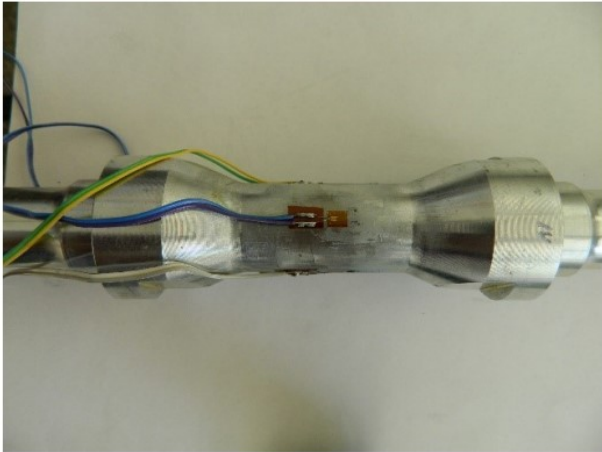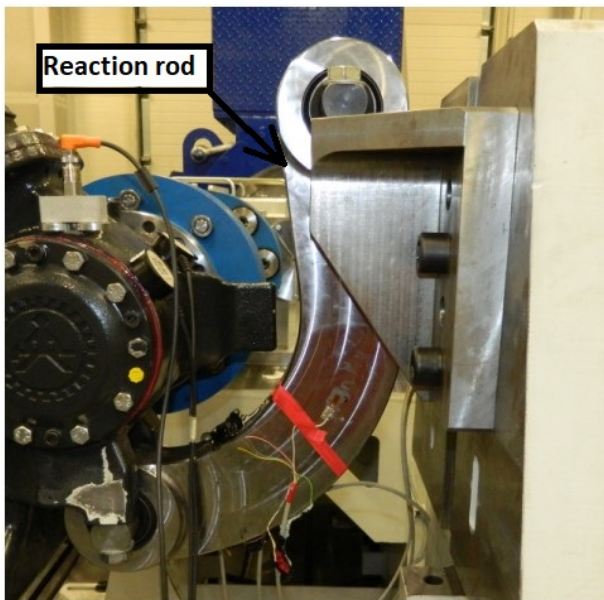
FIGURE 6. Instrumented reaction rod of tramcar 14T [9].

FIGURE 7. Instrumented reaction rod of a metro car [9].

3. MEASUREMENTS

The measurements were realized so, that:

- Both rollers were smeared with a soap, see Figure 11,

- Rollers were accelerated by driven wheel-set,

- When the smeared surfaces came into the contact with wheels the excessive slip occurred,

- Roller rig was stopped.

During this procedure the force in the reaction rod was measured. The value of the reaction rod force (S_1) was measured with the sampling frequency of 10 kHz. This measurement was carried out 20-times for three different vertical loads of the bogie to observe, what is the influence of the vertical load of the wheelset within the transitional phenomenon of the adhesion loss. At first the bogie was not externally loaded, which means that the axle load is approximately 148 kg due to the
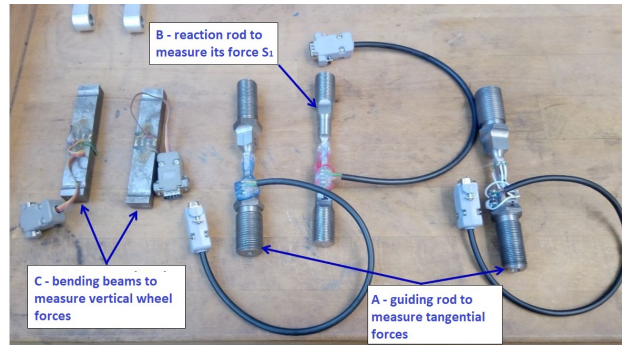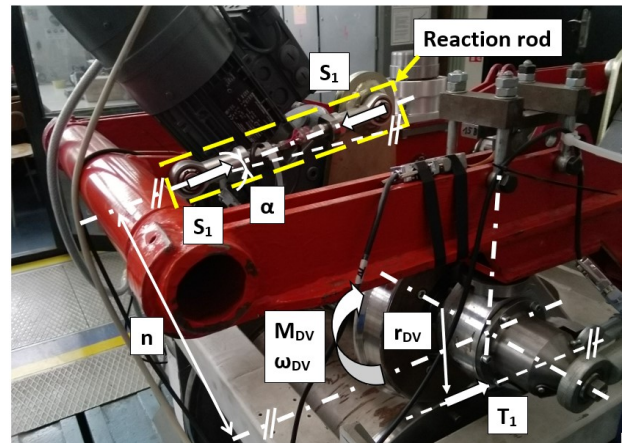

FIGURE 8. Measuring rods and beams [10].

FIGURE 9. Inclined reaction rod of roller rig.

mass of the driven wheelset, bogie frame etc. For other sets of measurement, the bogie frame was loaded via weights of 100 kg (Figure 12) and 200 kg. It means additional axle load of 50 kg and 100 kg respectively.

4. CONCEPTUAL DESIGN OF ACTIVE WHEELSET STEERING CONTROL

An example of a typical course of the measured force S_1 in the reaction rod within the measuring procedure is presented in Figure 13.

The detail of the adhesion loss itself is highlighted by the dashed square and depicted in Figure 14. Within the measured influence of the adhesion loss four parameters were assessed:

(1.) Δ_1 – the difference between the average value of the signal before the loss of the adhesion and during the reduced adhesion in the wheel-roller contact, see Equation (2).

(2.) Δ_2 – the difference between the average value of the signal during the reduced adhesion and after the regain of the adhesion in the wheel-roller contact, see Equation (3).

(3.) $\Delta_{1,A}$ – the maximal amplitude of the signal after the loss of the adhesion in the wheel-roller contact.

(4.) $\Delta_{2,A}$ – the maximal amplitude of the signal after the re-gain of the adhesion in the wheel-roller contact.
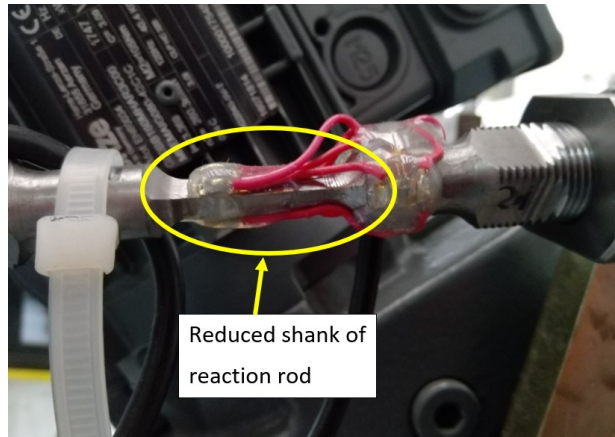
FIGURE 10. Reaction rod shank – detail.

FIGURE 11. Smeared rollers.

$$\Delta_1 = \overline{x}_{b\_l} - \overline{x}_{red\_ad}$$
$$= \frac{1}{n} \sum_{i=1}^{n} x_{i,b\_l} - \frac{1}{m} \sum_{j=1}^{m} x_{j,red\_ad}. \quad (2)$$

$$\Delta_2 = \overline{x}_{red\_ad} - \overline{x}_{reg\_ad}$$
$$= \frac{1}{m} \sum_{j=1}^{m} x_{j,red\_ad} - \frac{1}{p} \sum_{k=1}^{p} x_{k,reg\_ad}. \quad (3)$$

The parameters Δ_1 and Δ_2 were determined to see how the transition phenomena influence the nominal transferred force. The parameters $\Delta_{1,A}$ and $\Delta_{2,A}$ were determined to assess dynamic behaviour at the moment of the transition phenomena. Figure 15 presents determined values of Δ_1 (negative as decreased) and Δ_2 (positive as increased). It is clear, that they were not measured same values. Δ_2 reaches higher value of its arithmetic average 194 N and standard deviation of 21 N than Δ_1 with its arithmetic average of -179 N and standard deviation of 14 N. It is clearly visible, that Δ_2 shows bigger scatter of measured values.

Equivalent behavior with respect to arithmetic averages, when the adhesion is re-gained, can be also observed in case of assessed amplitudes for all three sets of measurements – Figure 16, 17, 18.
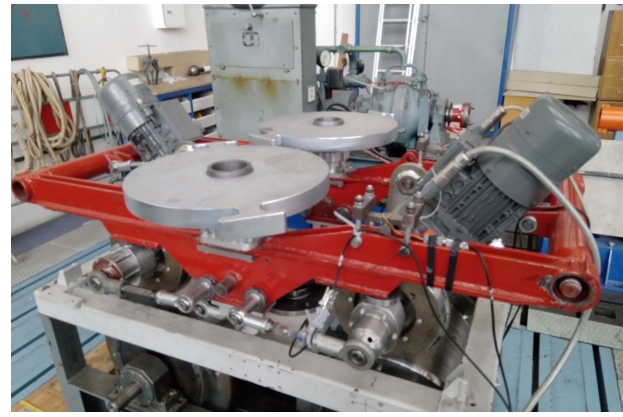

FIGURE 12. Loaded bogie frame by weights.

The assessment of amplitudes $\Delta_{1,A}$ and $\Delta_{2,A}$ also proved, that increasing of the axle load by app. 1/3 and 2/3 has influence on the dynamic behaviour of the force S_1. Specifically, the average values of amplitudes decrease as presented in Table 1. Standard deviations do not follow this trend exactly in case of the measurement for 100 kg.

Load	Arithmetic average		Standard deviation	
[kg]	$\Delta_{1,A}$	$\Delta_{2,A}$	$\Delta_{1,A}$	$\Delta_{2,A}$
0	120	190	36	50
100	111	170	30	38
200	104	150	29	48

TABLE 1. Basic statistic data of measured amplitudes.

5. CONCLUSION

Within the assessment of static parameters of Δ_1 and Δ_2 the measured values showed differences in terms of average values and their standard deviation as well. It means that Δ_2 reaches higher values and its scatter is also higher, than in the case of values of Δ_1. The evaluation of the behaviour of this parameter indicates, that re-gain of adhesion is more dynamic transition phenomenon than the loss of the adhesion. Equivalent evaluation can be done also with respect to the parameters of $\Delta_{1,A}$ and $\Delta_{2,A}$, where the average value is also bigger in the case of the re-gain of the adhesion. The assessment of the amplitudes indicates the influence of the axle load too. It can be stated, that when the axle load increases the dynamics of the transition phenomena decreases for both, the loss of the adhesion and the re-again of the adhesion. So higher axle load has positive influence on the dynamic overloading of the mechanical part of the traction drive system, which is caused by this kind of transition phenomenon.

LIST OF SYMBOLS
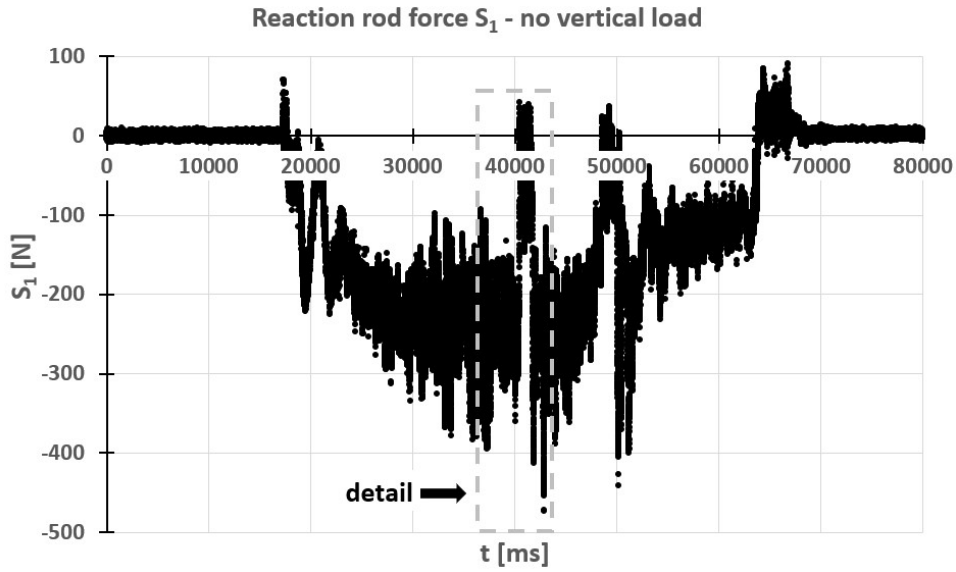M_H　Shaft torque [N]
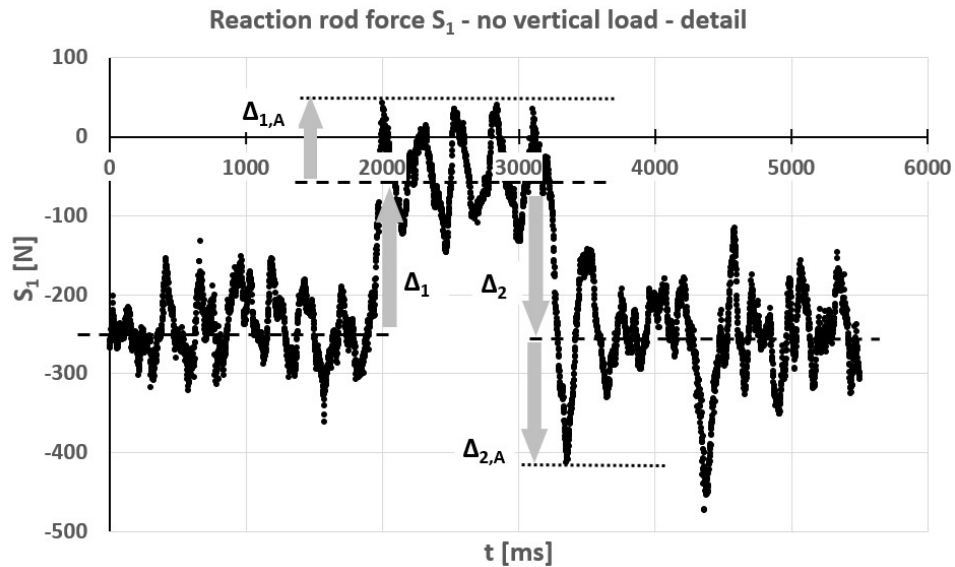M_M　Motor torque [N]

FIGURE 13. Course of reaction rod S_1.

FIGURE 14. Adhesion loss impact within force S_1 – detail.
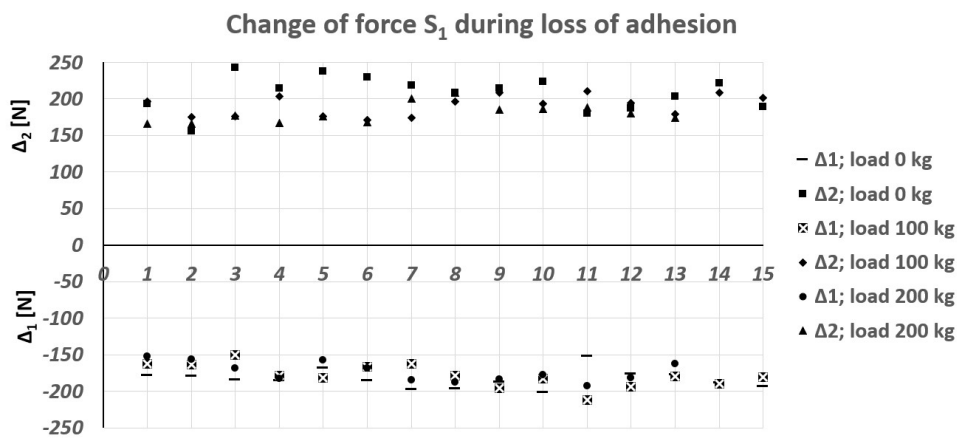

FIGURE 15. Change of force S_1 – all vertical bogie loads.

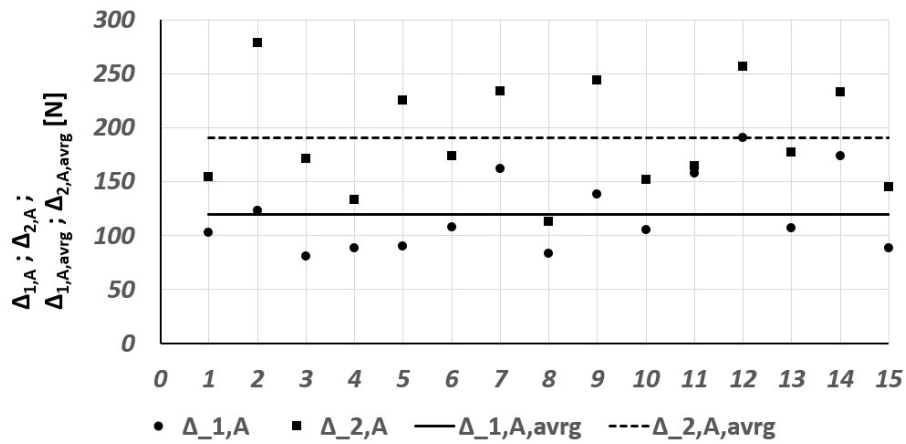**Amplitude of force S$_1$ during loss and renewal of adhesion - load 0 kg**

FIGURE 16. Amplitudes of force S_1 – no vertical bogie load.

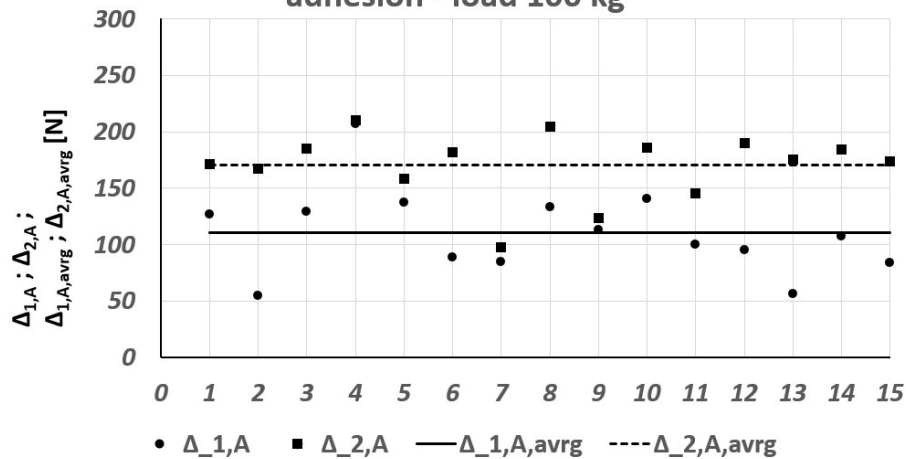**Amplitude of force S$_1$ during loss and renewal of adhesion - load 100 kg**

FIGURE 17. Amplitudes of force S_1 – 100 kg vertical bogie load.

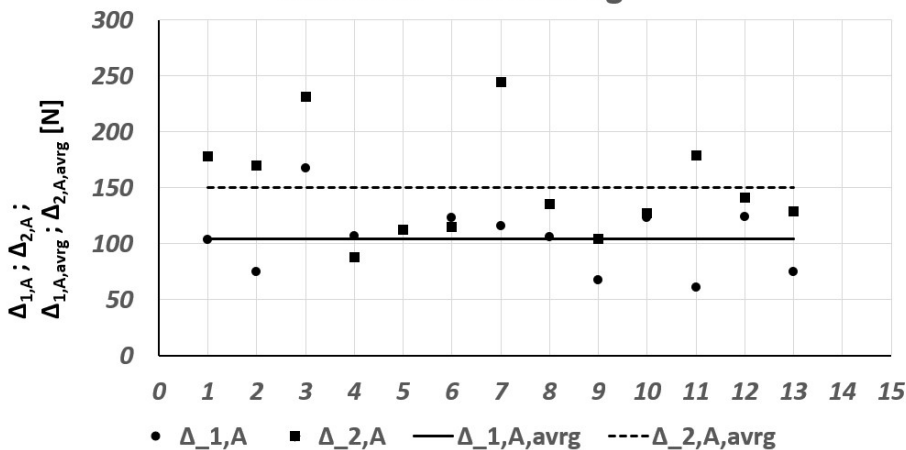**Amplitude of force S$_1$ during loss and renewal of adhesion - load 200 kg**

FIGURE 18. Amplitudes of force S_1 – 200 kg vertical bogie load.

n Arm of S_1 force [m]

$r_{DV} or r_k$ Wheelset/wheel radius [m]

$S or S_1$ Reaction rod force [N]

$T or T_1$ Wheelset-roller force [N]

x_{i,b_l} Value of signal before loss of adhesion [N]

$\overline{x}_{b\_l}$ Arithmetic average of signal before loss of adhesion [N]

x_{j,red_ad} Value of signal during reduced adhesion [N]

$\overline{x}_{red\_ad}$ Arithmetic average of signal during reduced adhesion [N]

x_{k,reg_ad} Value of signal after regaining of adhesion [N]

$\overline{x}_{reg\_ad}$ Arithmetic average of signal after regaining of adhesion [N]

Z Horizontal distance [m]

α Reaction rod angle [°]

Δ_1 Decrease of S_1 force [-]

Δ_2 Increase of S_1 force [-]

$\Delta_{1,A}$ Max. amplitude of S_1 force [-]

$\Delta_{2,A}$ Max. amplitude of S_1 force [-]

References

[1] R. Lal. Selection of suspension arrangement of traction motors : A right approach. [2019-09-07], `https://www.yumpu.com/en/document/view/21978467/selection-of-suspension-arrangement-of-traction-motors-a-rdso`.

[2] J. Kolář. *Teoretické základy konstrukce kolejových vozidel*. Česká technika – nakladatelství ČVUT, 2009.

[3] O. Suchánek. Návrh závěsky u nápravové převodovky příčného částečně odpruženého pohonu dvojkolí. Bachelor Thesis, FME CTU in Prague, 2019, [2022-04-21], `https://dspace.cvut.cz/handle/10467/84788`.

[4] M. W. Winterling. *Oscillations in rail vehicle*. Delft University Press, Mekeleg 4, 2628 CD Delft, The Netherlands, 1997.

[5] R. Schneider. Torsionsschwingungen von Radsatzwellen – Systemanalyse Teil 1: System- und Modellbeschreibung. *ZEVrail* **141**(11/12):452–461, 2017.

[6] R. Schneider. Torsionsschwingungen von Radsatzwellen – Systemanalyse Teil 2: Physikalische Untersuchungen und Sicherheitsbetrachtung. *ZEVrail* **142**(01/02):27–36, 2018.

[7] J. Kolář. Dynamika individuálního pohonu dvojkolí s nápravovou převodovkou. In *XX. Medzinárodná konferencia – Súčasné problémy v kolajových vozidlech, Žilina*, pp. 139–148. 2011.

[8] T. Fridrichovský. Dynamické vlastnosti pohonů moderních kolejových vozidel. Doctoral thesis, FME CTU in Prague, 2022, [2022-04-21], `https://dspace.cvut.cz/handle/10467/99978`.

[9] M. Dub. Analýza možností autodiagnostiky pohonů kolejových vozidel. Doctoral thesis, CTU in Prague, 2016.

[10] V. Dybala, P. Bauer, T. Fridrichovský. Využití tenzometrie pro měření součinitele adheze na kladkovém stavu ČVUT. *Nová železniční technika* **2021**(1):26–29, 2021.